



Removal of Cd(II) onto *Raphanus sativus* peels biomass: equilibrium, kinetics, and thermodynamics

Muhammad Aqeel Ashraf^{a,c,*}, Muhammad Abdur Rehman^b, Yatimah Alias^a, Ismail Yusoff^c

^aDepartment of Chemistry, University of Malaya, Kuala Lumpur 50603, Malaysia

^bAnalytical Chemistry Division, Institute of Chemical Sciences, Bahauddin Zakariya University, Multan 60800, Pakistan

^cDepartment of Geology, University of Malaya, Kuala Lumpur 50603, Malaysia
Tel. +60 172770972; Fax: +60 379675149; email: chemark786@gmail.com

Received 10 October 2012; Accepted 19 November 2012

ABSTRACT

Raphanus sativus peels (RSP) biomass for the adsorptive removal of Cadmium (II) has been studied. The effect of different experimental parameter like pH, temperature, contact time, and initial concentration has been reported. The equilibrium adsorption data were subjected to different adsorption isotherms (Langmuir, Freundlich, Dubinin-Radushkevich, Temkin, Flory-Huggins isotherm, and Brunauer, Emmet and Teller isotherms), for kinetic studies pseudo-first-order, pseudo-second-order, Banghams's model, and intraparticle diffusion kinetic models were applied. The experimental results indicated that the adsorption of Cd(II) followed monolayer adsorption model and pseudo-second-order kinetics. The change in thermodynamic parameters like free energy (ΔG°), enthalpy (ΔH°), and entropy (ΔS°) was also evaluated. It was found that the RSP exhibits good adsorption capacity for Cadmium (II) from aqueous solution.

Keywords: *Raphanus sativus*; Bioadsorbent; Kinetics; Thermodynamics; Equilibrium; Cadmium (II)

1. Introduction

The environment sustainability is a serious public health issue due to a long list of pollutants from a number of sources. Among these the heavy metals are in the worst case due to their toxicity, bioaccumulation, and persistent nature. Cadmium is a toxic metal from the nonessential category of metals for life, it causes hypertension, bone lesions, and lungs malfunction. Cadmium ions can replace Zn(II) ions in some metalloenzymes, thereby affecting the enzyme activity

[1]. It is incorporated into the safe aquifer from a number of anthropogenic sources including mining activities, pigments developments, electroplating, alloys making, and batteries processing industries [2]. It has the ability to block essential functional groups of biomolecules, replacing essential metals, and destroying the integrity of biomembranes [3].

Developing technically simple and economically efficient methods of industrial waste purification is one of the challenges of the twenty-first century [4]. Many chemical methods such as chemical precipitation [5], electroflotation [6], ion exchange [7], and

*Corresponding author.

reverse osmosis [8] have been used for the removal of heavy metals. However, these processes are economically nonfeasible especially in developing countries. The adsorption process has been found to be economically appealing for the removal of heavy metals with better removal efficiency from wastewater [9]. The first step is the optimization of these adsorption methods to suite in terms of its selectivity and demand of particular industrial wastewater contaminants. In the light of cost and benefit analysis, different types of biomasses or adsorbents of natural origin have been studied for the last two decades and adsorption characteristics of many of them have been thoroughly investigated [10,11].

Biosorption is an innovative technology for heavy metal removal from industrial wastewater; it is used as an alternative to conventional methods such as chemical precipitation, ion exchange, and chelation by synthetic resins, membrane filtration, and adsorption onto activated carbon. The agroindustrial wastes seem to be the most promising due to its low cost and large abundance in nature.

Algerian Cork with maximum adsorption capacity 9.65 mg/g [12], Castor Hull 6.98 mg/g [13], Tea industry waste 11.26 mg/g [14], Olive cake 10.56 mg/g [15], Citrus Peels 43.12 mg/g (0.40 mmol/g) [16], *Pinus halepensis* sawdust 7.35 mg/g [17], Activated sludge biomass 0.358 mmol/g, (38.62 mg/g) [18], *Enteromorpha compressa* 9.50 mg/g [19], *Nostoc commune* 126.32 mg/g [20], Oak bar char 5.40 mg/g [21], *Rhizopus arrhizus* 26.8 mg/g [22], pretreated *Phanerochaete chrysosporium* 15.2 mg/g [23], *Ulva lactuca* 29.2 mg/g [24], *P. chrysosporium* 23.0 mg/g [25], and *Amanita rubescens* 27.3 mg/g [26] have been reported in literature.

Agricultural by-products are mainly made up of lignin and cellulose, and are rich in different kinds of functional groups such as alcohols, aldehydes, ketones, carboxylic, phenols, and ethers. These groups have the ability to bind heavy metals by forming complexes with ionic species in solution via donation of an electron pair by the functional group on the biosorbent. *Raphanus sativus* peel (*RSP*) is a new adsorbent to be explored from the adsorption point of view. In the literature, there were reports on the bioaccumulation of Cd(II) onto *RSP* [27] but to the best of our knowledge no reports were found regarding its use as a bioadsorbent for Cadmium (II).

2. Material and methods

2.1. Preparation of *RSP* bioadsorbent

R. sativus were obtained from the local market of Multan, Pakistan. It was washed with deionized water to remove any particles of dirt or dust on its surface.

The peels were taken off, cut into small pieces, and placed in the sun for one day to dry. The petridishes containing sun-dried peels were placed in an electric oven at 100°C for another 24 h to make them moisture free. The dried peels biomass was ground in electric grinder into fine particle size. The particle-size fractionation was done by sieving to obtain particles with average diameter of 0.1–0.3 mm.

2.2. Adsorption studies

Cadmium nitrate ($\text{Cd}(\text{NO}_3)_2 \cdot 4\text{H}_2\text{O}$, >99.9%), was obtained from Merck (Germany) was used as adsorbate and *RSP* was used as adsorbent. A stock solution of cadmium (100 mg L^{-1}) was prepared by dissolving $\text{Cd}(\text{NO}_3)_2 \cdot 4\text{H}_2\text{O}$ in doubly distilled water. The solutions of different concentrations i.e. 0.3, 0.5, 1.0, 3.0, 5.0, and 10.0 mg L^{-1} were prepared by successive dilutions with the same solvent. These were used as standards to make calibration curve using Flame Atomic Absorption Spectrophotometer (FAAS). A weighed amount of 0.1 g of *RSP* was added in a flask containing 20 mL of Cd(II) solution of known concentration and was shaken in a thermostat shaker at a rate of $100 \text{ strokes min}^{-1}$ at a temperature of 333 K for 120 min. The pH of the solution was 7.0. After shaking, the solution was filtered through a Millipore filter paper of $0.45 \mu\text{m}$, with the aid of a suction pump, collected in a vial and feed to the FAAS analysis.

The amount of Cd(II) adsorbed onto *RSP* was calculated using the following equation.

$$q_e = \frac{(C_0 - C_e)V}{m} \quad (1)$$

where C_0 is the initial Cd(II) concentration (mg L^{-1}), C_e is the equilibrium concentration (mg L^{-1}), V is the volume of the solution (L), and m is the mass (g) of *RSP*.

2.3. Kinetics of Cd(II) adsorption

For the optimization of the shaking time, 20 mL of aqueous solution (10 mg L^{-1}) of Cd(II) was taken into conical flasks and the fixed amount of *RSP* (0.1 g) was added. The labeled flasks were taken out after different time interval from the shaker, filtered, and placed in a vial to be further studied on FAAS. It has been observed that adsorption of Cd(II) increased with increasing the shaking time and attained a constant value at equilibrium after a specific time. The optimum shaking time was found to be 120 min which was used for all further adsorption studies.

3. Results and discussion

3.1. FTIR results of RSP biomass

Fourier transformed infrared (FTIR) analytical technique was used to identify the presence of characteristic functional groups on RSP biomass involved in the adsorption process. The FTIR spectrum is shown Fig. 1. The following peaks: broad hydroxyl peak at $3,500\text{ cm}^{-1}$, strong peaks at $1,646\text{--}1,650\text{ cm}^{-1}$ corresponding to the C=O and C=C stretching adsorption bonds indicating the abundance of these functional groups on the RSP waste biomass.

3.2. Adsorption isotherms

The adsorption isotherms for Cd(II) removal were studied at 313, 323, and 333 K to study the adsorption capacity of the RSP with the changes in the medium temperature.

3.2.1. Freundlich isotherm

The linear form of Freundlich model is given by Eq. (2):

$$\ln q_e = \ln K_F + \frac{1}{n} \ln C_e \quad (2)$$

where q_e is the equilibrium amount of Cd(II) adsorbed (mg g^{-1}), K_F is the Freundlich constant associated with the degree of adsorption [28], and n is the heterogeneous factor and related to the intensity of adsorption. The value of $1/n$ equal to unity indicates the adsorption process is linear, whereas its value above unity represents the physical adsorption and below unity refers to chemical adsorption [29]. The closer its value to zero implies that the adsorbent surface is more heterogeneous. Fig. 2 shows the Freundlich isotherms while the parameters K_F and n were calculated from intercept and slopes, respectively, which are given in Table 1. The Freundlich constant K_F value for adsorption of Cd(II) showed the process to be more favorable.

3.2.2. Langmuir isotherm

The Langmuir adsorption isotherm is given by Eq. (3).

$$\frac{C_e}{q_e} = \frac{1}{K_L} + a_L \frac{C_e}{K_L} \quad (3)$$

where K_L represents the energy of adsorption and a_L shows the binding force between adsorbate and adsorbent [11]. Langmuir curve is shown in Fig. 3.

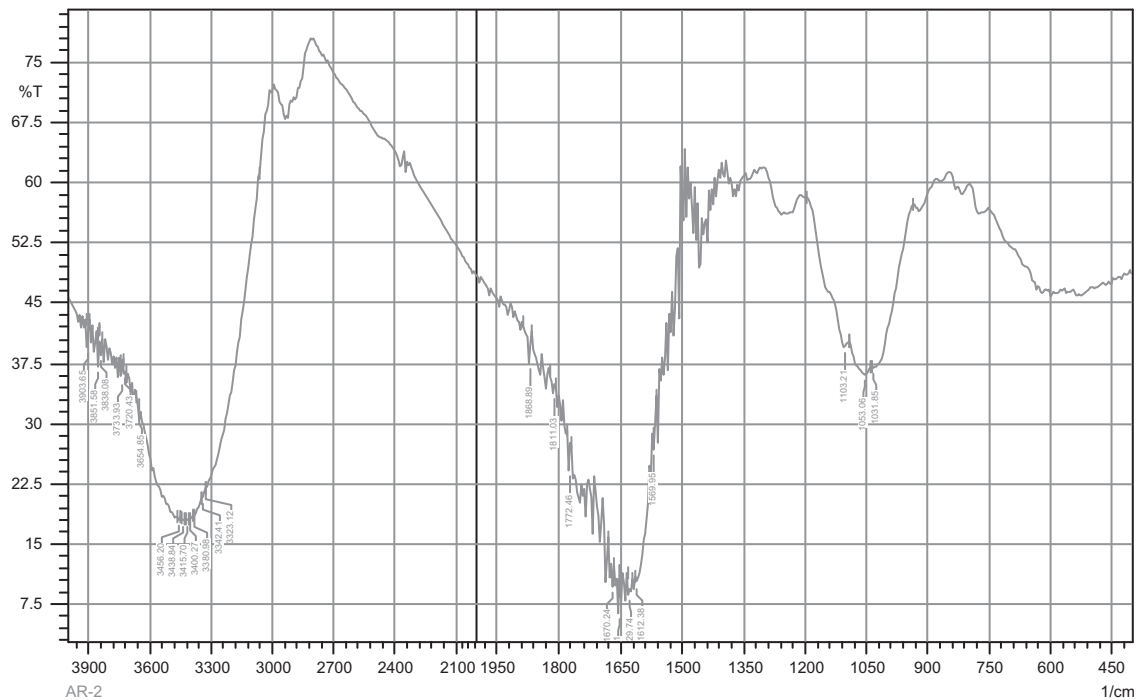


Fig. 1. FTIR spectrum of RSP biomass.

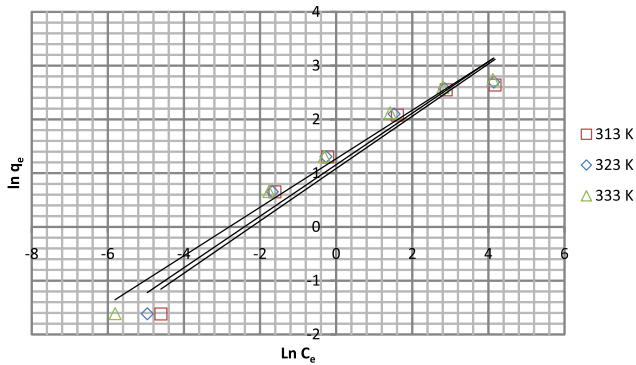


Fig. 2. Freundlich isotherm for Cd(II) adsorption onto RSP at 333 K.

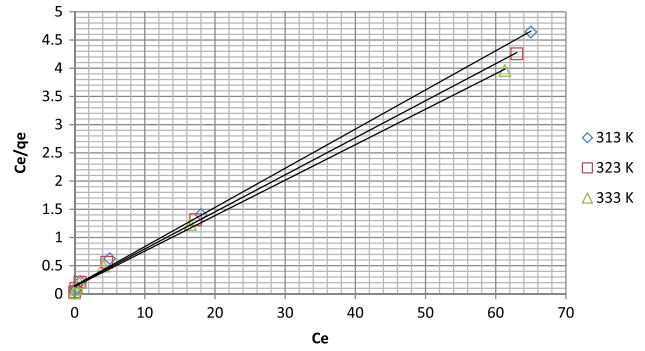


Fig. 3. Langmuir isotherms for Cd(II) adsorption onto RSP at 313 K.

Table 1
A comparison among the isotherms constants for Cd(II) adsorption onto RSP at 313 K, 323 K, and 333 K

Adsorption model	313 K	323 K	333 K
<i>Langmuir</i>			
q_m (mg/g)	14.406	15.226	15.903
K_L (L/g)	6.915	7.151	7.711
a_L (L/mg)	0.480	0.470	0.485
R_L	0.126	0.123	0.115
R^2	0.999	0.999	0.999
<i>Freundlich</i>			
n	2.054	2.087	2.215
K_F (mg/g)	2.962	3.181	3.555
R^2	0.972	0.978	0.987
<i>Temkin</i>			
K_T (L/g)	35.240	43.145	74.982
B_t (mg/g)	1.720	1.731	1.634
R^2	0.956	0.948	0.929
<i>Dubinin-Radushkevich</i>			
X_m (mg/g)	7.465	7.535	7.447
K_{DR}	0.027	0.023	0.017
E (kJ/mol)	4.306	4.634	5.444
R^2	0.932	0.926	0.915
<i>F-H Model</i>			
n	-1.298	-1.204	-1.011
K_{FH}	0.080	0.083	0.094
R^2	0.992	0.990	0.976
<i>BET model</i>			
X_m	54.434	68.466	115.422
c	1.003	1.002	1.001
R^2	0.852	0.900	0.953

The adsorption capacity of RSP can be calculated by the following Eq. (4) [30]:

$$q_m = \frac{K_L}{a_L} \tag{4}$$

The dimensionless separation factor R_L can be calculated using Eq. (5):

$$R_L = \frac{1}{1 + K_L C_e} \tag{5}$$

The Langmuir parameters q_m , K_L , R_L , and a_L are given in Table 1.

The R_L parameter describes whether the adsorption process is favorable:

$R_L > 1$ (Unfavorable); $R_L = 1$ (Linear); $0 < R_L < 1$ (Favorable); $R_L = 0$ (Irreversible).

The R_L parameter is less than 1 but greater than 0, confirming the adsorption process to be favorable.

3.2.3. Temkin isotherm

Temkin equation is based on the assumption that heat of adsorption of all the molecules in the layer decreases linearly with coverage due to adsorbate–adsorbent interactions. According to Temkin, adsorption is characterized by a uniform distribution of binding energies up to some maximum value [31].

The linear form of Temkin equation is given as:

$$q_e = B_t \ln K_T + B_t \ln C_e \tag{6}$$

where K_T is the equilibrium binding constant corresponding to the maximum binding energy and B_t is related to the heat of adsorption [32]. The value of K_T and B_t are obtained from the intercept and slope of the plot of q_e vs. $\ln C_e$ respectively as given in Fig. 4. and their values are tabulated in Table 1.

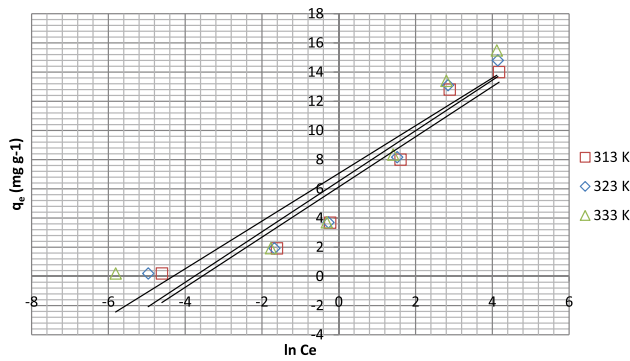


Fig. 4. Temkin isotherms for Cd(II) adsorption onto RSP.

3.2.4. Dubinin-Radushkevich (D-R) isotherm

D-R isotherm [33] is applied to the adsorption data and is used in the following linear form:

$$\ln q_e = \ln X_m - \beta \epsilon^2 \tag{7}$$

where X_m represents the maximum sorption capacity of the *R. sativus* (mg g^{-1}), β is a constant related to adsorption energy, and ϵ is Polanyi adsorption potential [34], the amount of energy required to pull an adsorbed molecule from its adsorption space to infinity which can be calculated using the following equation:

$$\epsilon = RT \ln \left(1 + \frac{1}{C_e} \right) \tag{8}$$

where R is the universal gas constant in $\text{kJ mol}^{-1} \text{K}^{-1}$, T is the temperature in Kelvin while q_e is the equilibrium concentration of Cd(II) in solution (mg L^{-1}). Polanyi theory [35] is based upon the fact that the adsorption potential is related to an excess of sorption energy over the condensation energy, it is independent of temperature. The plots of $\ln q_e$ vs. ϵ^2 follow linearity as shown in Fig. 5. The values of β and X_m calculated from the slopes and intercepts, respectively, are listed in Table 1.

The values of adsorption energy E [32] can be computed using the following relationship:

$$E = \frac{1}{\sqrt{-2\beta}} \tag{9}$$

3.2.5. Flory-Huggins isotherm (F-H)

The F-H model was selected to account for the degree of surface coverage characteristics of the adsorbate on the adsorbent. The linear form of F-H equation is represented by:

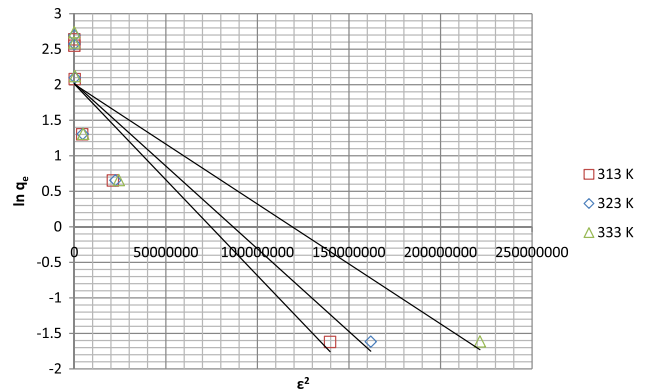


Fig. 5. D-R isotherms for Cd(II) adsorption onto RSP.

$$\log \frac{Q}{C_i} = \log K_{FH} + n \log(1 - Q) \tag{10}$$

where Q is the degree of surface coverage and it can be calculated by the following equation:

$$Q = 1 - \frac{C_e}{C_i} \tag{11}$$

While n is the number of adsorbate molecules occupying the adsorption sites, K_{FH} is the equilibrium constant. The n and K_{FH} constants (Table 1) were calculated from the slope and intercept of the curve $\log Q/C_i$ vs. $\log(1 - Q)$ as shown in Fig. 6.

3.2.6. BET model

The multilayer adsorption can be explained by Stephen Brunauer, Paul Emmet, and Edward Teller (BET isotherm).

$$\frac{C_e/C_0}{q_e(1 - C_e/C_0)} = \frac{C}{X_{\max}C} + \frac{C - 1}{X_{\max}C} \cdot \frac{C_e}{C_0} \tag{12}$$

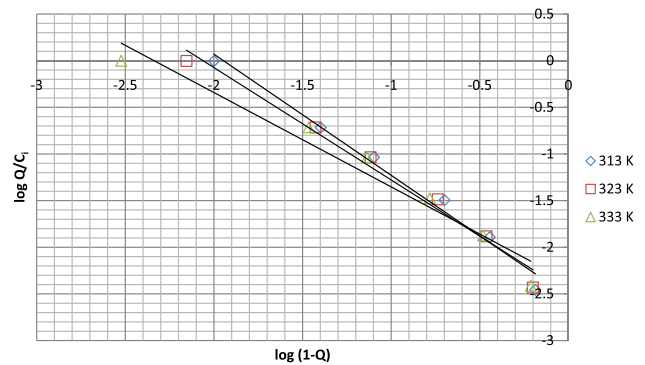


Fig. 6. F-H isotherm for Cd(II) adsorption onto RSP.

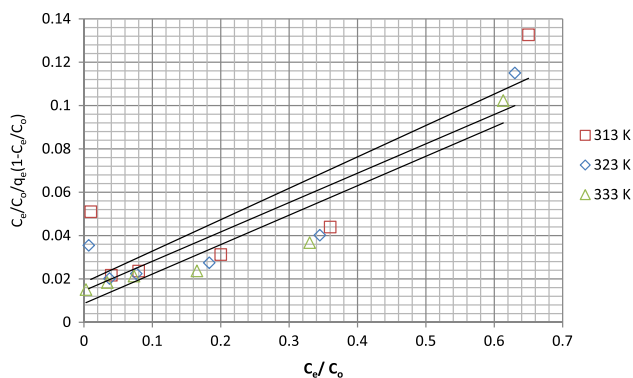


Fig. 7. BET isotherms for the Cd(II) adsorption onto RSP.

where C_0 is the initial and C_e is the equilibrium concentration of the Cd(II), C is a constant related with the heat of adsorption. X_{\max} is the maximum adsorption at monolayer coverage and it could be calculated from the slope and intercept of the plot between C_e/C_0 vs. $C_e/C_0/q_e(1 - C_e/C_0)$, its values are given in the Table 1 as calculated from the slope and intercept in Fig. 7.

3.3. Effect of pH

The role of pH during the adsorption of Cd(II) onto RSP was determined from 2.0 to 9.0 at Cd(II) concentration 10.0 mg L^{-1} , adsorbent dose 0.1 g and Shaking time 120 min at 100 rpm at 333 K as given in Fig. 8. The percent removal increased from 49 to 86% as the pH of the medium increased from 2.0 to 9.0. Adsorption capacity of adsorbent, surface charges, and active sites might be attributed to the adsorption behavior of the adsorbent at various pH values. The surface of RSP contains large number of active sites as confirmed by FTIR analysis. The higher basic pH values of the solution lead towards precipitation of Cd(II) in the form of Hydroxides so higher pH was not selected for subsequent studies.

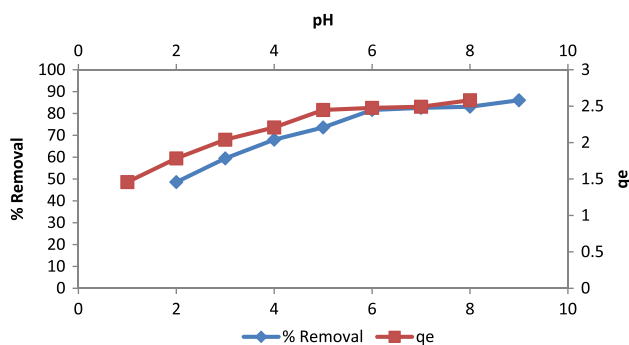


Fig. 8. Effect of pH on the adsorption of Cd(II) onto RSP.

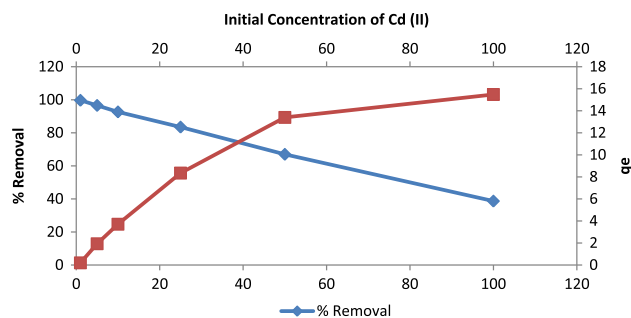


Fig. 9. Effect of Cd(II) initial concentration on its adsorption on RSP biomass.

3.4. Effect of cadmium (II) concentration

The concentration range of Cd(II) selected was from 1.0 to 100.0 mg L^{-1} , the q_e value increased from 0.1994 to 15.480 mg g^{-1} and the percentage removal decreased from 99.7 to 38.7% at 333 K as shown in Fig. 9. It is because of the fact that at lower concentration there is relatively less competition for the vacant position at the RSP active surface sites for adsorption between the Cd (II) ions, while there is more competition at higher concentration so the % age removal decreases [36].

3.5. Kinetics of Cd(II) adsorption onto RSP

The dynamics of adsorption of Cd(II) onto RSP was evaluated by employing the following kinetic models: pseudo-first-order, pseudo-second-order, intraparticle diffusion, and Banghams model. In both pseudo-first-order and pseudo-second-order models, all the steps of adsorption are lumped together. Overall adsorption rate is proportional to the driving force, concentration gradient, in case of the first order, while in the case of the second order, it is proportional to the square of driving force [35].

3.5.1. Pseudo-first-order model

The linear form of pseudo-first-order model is given by Eq. (13) [11].

$$\ln(q_e - q_t) = \ln q_e - k_1 t \quad (13)$$

where k_1 , is the first-order rate constant of adsorption, while q_e and q_t are the maximum amount adsorbed at equilibrium and at time t , respectively. The linear plots of $\ln(q_e - q_t)$ vs. t yield straight lines is given in Fig. 10.

The values of k_1 (min^{-1}) and q_e (mg g^{-1}) computed from the slope and intercept of the pseudo-first-order linear plots are depicted in Table 2.

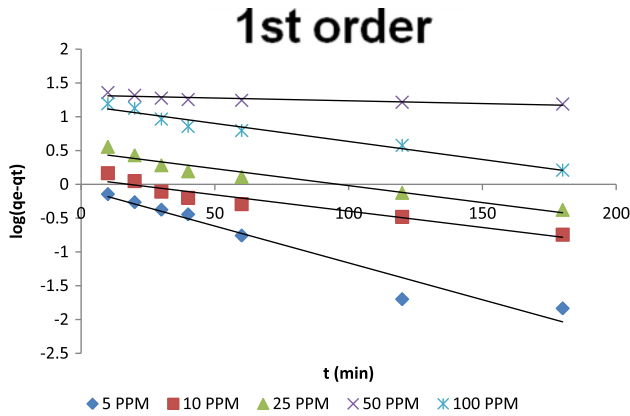


Fig. 10. Pseudo-first-order plot for Cd(II) adsorption onto RSP biomass.

3.5.2. Pseudo-second-order model

The linear form of pseudo-second-order model is given by Eq. (14) [37]:

$$\frac{t}{q_t} = \frac{1}{k_2 q_e^2} + \frac{t}{q_e} \tag{14}$$

where k_2 ($\text{g mg}^{-1} \text{min}^{-1}$) is the rate constant of pseudo-second-order kinetic equation, it can be calculated from

the intercept of the linear plot of time vs. t/q_t . While the equilibrium adsorption capacity q_e can be calculated from the slope of this linear plot as shown in Fig. 11.

The calculated (cal) value of k_2 ($\text{g mg}^{-1} \text{min}^{-1}$) and q_e (mg g^{-1}) are given in the Table 2.

According to correlation coefficient values, the second-order model is found to be more suitable to describe the adsorption kinetic data than that of

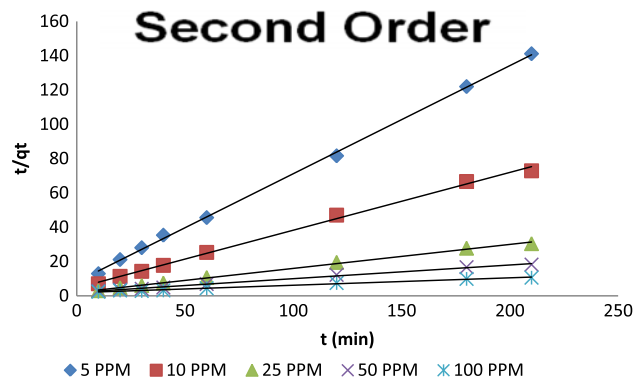


Fig. 11. Pseudo-second-order plot for Cd(II) adsorption onto RSP biomass.

Table 2

A comparison among the parameters of kinetic models for the Cd(II) adsorption onto RSP at 5, 10, 25, 50, and 100 mg/L of initial concentration

C_0 (mg/L)	5	10	25	50	100
<i>Pseudo-first-order</i>					
q_e (exp.)/ mg g^{-1}	1.488	2.880	6.901	11.516	19.816
q_e (cal.)/ mg g^{-1}	0.930	1.091	1.621	3.739	3.218
k_1 (min^{-1})	0.025	0.011	0.012	0.002	0.012
R^2	0.974	0.965	0.971	0.873	0.980
<i>Pseudo-second-order</i>					
q_e (cal.)/ mg g^{-1}	1.587	2.969	7.147	12.520	23.099
k_2 ($\text{g mg}^{-1} \text{min}^{-1}$)	0.048	0.025	0.010	0.003	0.001
h ($\text{mg g}^{-1} \text{min}^{-1}$)	0.122	0.218	0.501	0.498	0.538
$t_{1/2}$ /min	13.031	13.654	14.280	25.160	42.956
R^2	0.999	0.999	0.999	0.998	0.995
<i>Intraparticle diffusion</i>					
I (cal.)/ mg g^{-1}	0.711	0.711	3.162	3.182	2.471
K_{id} ($\text{g mg}^{-1} \text{min}^{-1}$)	0.060	0.108	0.267	0.603	1.237
R^2	0.940	0.939	0.942	0.935	0.9574
<i>Banghams's model</i>					
K_0	0.396	0.470	0.591	0.520	0.493
q_t	0.600	0.403	0.331	0.340	0.493
R^2	0.991	0.982	0.985	0.953	0.957

the first-order model for the Cd(II) on *R. sativus*. Furthermore, the calculated equilibrium adsorption capacity q_e (mg g^{-1}) Table 2 is in good agreement with the experimental values for the second-order model. On the basis of these evidences, it has been confirmed that the adsorption process is showing pseudo-second-order kinetic behavior.

Based on the second-order best fit model, the initial sorption rate (h) and half adsorption time ($t_{1/2}$) are calculated from Eqs. (16) and (17), respectively, and listed in Table 2 [38].

$$h = k_2 q_e^2 \quad (15)$$

$$t_{1/2} = \frac{1}{k_2 q_e} \quad (16)$$

3.5.3. Intraparticle diffusion model

Fick's second law was used to evaluate the experimental data, to see the possibility of intraparticle diffusion as the rate limiting step, it is given by the Eq. (17) [34].

$$q_t = k_{id} t_{1/2} + I \quad (17)$$

where k_{id} ($\text{mg g}^{-1} \text{min}^{-1/2}$) is the intraparticle diffusion rate constant and I is the boundary layer effect (mg g^{-1}). The value of I is directly proportional to the boundary layer thickness. According to Eq. (17), the plot of q_t vs. $t_{1/2}$ should be a straight line with a slope k_{id} and intercept I when the mechanisms follows the intraparticle diffusion model [39]. Fig. 12. shows the plot of q_t vs. $t_{1/2}$ for the adsorption and the values of I and k_{id} are given in Table 2.

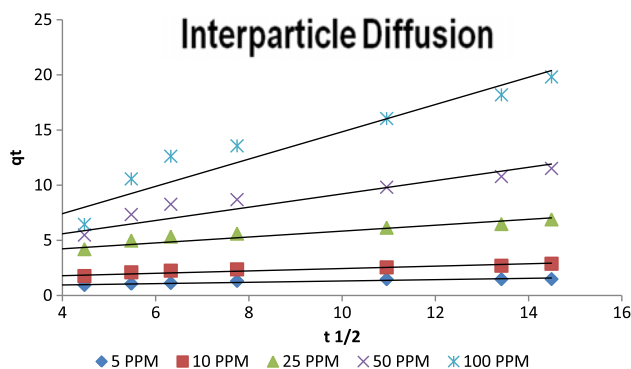


Fig. 12. Intraparticle diffusion plot of Cd(II) on RSP biomass.

According to Ho [40], it is essential for the q_t vs. $t_{1/2}$ plot to go through the origin if the intraparticle diffusion is the rate limiting step.

Value of I (Table 2) shows deviation of line from the origin, which indicates that the surface adsorption and intraparticle diffusion are simultaneously operating during the adsorption of Cd(II) onto RSP.

3.5.4. Banghams's model

Kinetic data were also evaluated with Banghams's equation [41] to determine the slowest step during the adsorption.

$$\log\left(\log\left(\frac{C_0}{C_0 - q_t m}\right)\right) = \log\left(\frac{k_0 m}{2.303 V}\right) + \alpha \log(t) \quad (18)$$

where V is the volume of solution (l) and α and k_0 are constants. The Banghams plot shows a nonlinear curve for Cd(II) onto *R. sativus*, indicating that the diffusion of adsorbate into pores of the sorbent is not the only rate determining step [31,42] and is depicted in Fig. 13. It seems that film and pore diffusion were also significantly contributing towards the overall diffusion mechanism. The values of constant α and k_0 are given in Table 2.

The comparison of maximum adsorption capacities of *R. sativus* with other bioadsorbents represents its effectiveness for Cd(II) removal from aqueous solutions which is illustrated in Table 3.

3.6. Thermodynamics study—effect of temperature

The effect of changes in temperature during the adsorption of Cd(II) onto RSP was studied to determine

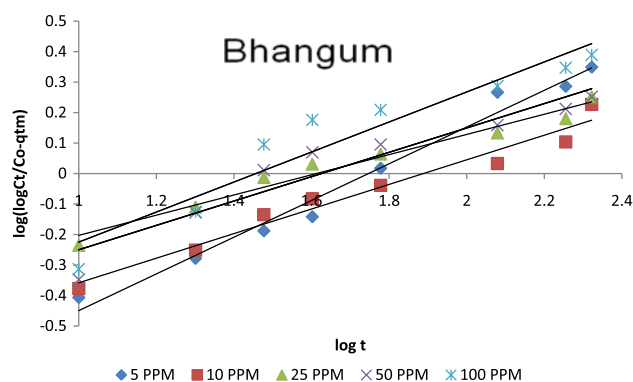


Fig. 13. Banghams's plots for the adsorption of Cd(II) onto RSP.

Table 3
Maximum adsorption capacities of other bioadsorbents for Cd(II) for aqueous media

Adsorbents	q_{\max} (mg/g)	References
Algerian cork	9.65	[12]
Tea industry waste	11.26	[14]
Olive cake	10.56	[15]
<i>P. halepensis</i> sawdust	7.35	[17]
Oak bar char	5.40	[21]
<i>R. arrhizus</i>	26.8	[22]
Pretreated <i>P. chrysosporium</i>	15.2	[23]
<i>U. lactuca</i>	29.2	[24]
<i>P. chrysosporium</i>	23.0	[25]
<i>A. rubescens</i>	27.3	[26]
RSP	19.82	Present study
Activated sludge biomass	38.62	[18]
Castor hull	6.98	[13]
Citrus peels	43.12	[16]
<i>E. compressa</i>	9.50	[19]
<i>N. commune</i>	126.32	[20]

the nature of the process. The adsorption capacity increased with temperature from 293 to 333 K. This indicated the endothermic nature of the process. The values of free energy (ΔG°), enthalpy (ΔH°), and entropy (ΔS°) were calculated using following equations and their values are given in Table 4:

$$\Delta G = -RT \ln K_D \quad (19)$$

$$\ln K_D = \frac{\Delta S^\circ}{R} - \frac{\Delta H^\circ}{RT} \quad (20)$$

where R is the universal gas constant ($8.3143 \text{ J mol}^{-1} \text{ K}^{-1}$). T is the temperature in Kelvin scale (K) and K_D is the distribution coefficient, calculated with the following equation:

$$K_D = \frac{q_e}{C_e} \quad (21)$$

Table 4
Thermodynamic constants for Cd(II) adsorption onto RSP at $C_0 = 10 \text{ mg L}^{-1}$

Temp. (K)	q_e (mg g ⁻¹)	K_D (L/g)	ΔG° (kJ mol ⁻¹)	ΔH° (kJ mol ⁻¹)	ΔS° (kJ mol ⁻¹ K ⁻¹)
293	2.50	0.67	-0.988	+5.844	+23.416
303	2.54	0.60	-1.272		
313	2.57	0.56	-1.520		
323	2.59	0.53	-1.717		
333	2.61	0.50	-1.930		

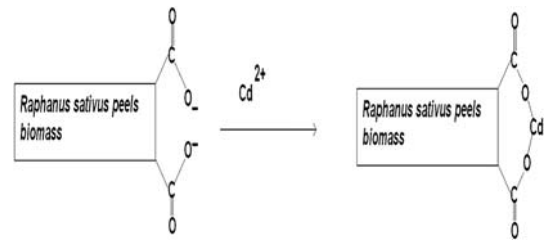


Fig. 14. Mechanism of Cd(II) adsorption onto RSP biomass.

where q_e (mg g⁻¹) is the equilibrium Cd(II) concentration adsorbed onto *R. sativus* and C_e (mg L⁻¹) is the equilibrium concentration of Cd(II) in the solution.

The negative value of ΔG represents the adsorption process of Cd(II) onto RSP is favorable and spontaneous in nature. The positive values of ΔH show the endothermic nature of adsorption process and its value $5.844 \text{ kJ mol}^{-1}$ indicates the possibility of physical adsorption [43]. The positive values of ΔS° show the increased disorder at the solid solution interface components. The increased adsorption capacity at higher temperatures was attributed to the enlargement of pore size and activation of the RSP surface.

3.7. Adsorption mechanism

The biosorption of Cd(II) onto *R. sativus* is through the functional groups present on the biomass. The principal functional groups as confirmed by FTIR analysis were the carboxylic groups which are depicted in Fig. 14. At acidic pH range, the carboxylic groups get protonated which results in lower metal uptake, because similar charges repel each other.

4. Conclusion

On the basis of experimental results, RSP waste biomass was capable of adsorbing the Cd(II) from aqueous solutions. The optimum parameters for equilibrium study were a contact time of 120 min, pH of 7, and RSP dose of 0.1 g/30 mL and a tem-

perature of 333 K. The maximum adsorption capacity (q_{\max}) was determined to be 19.82 mg/g under the optimum conditions. The adsorption of Cd(II) ions by *RSP* followed monolayer adsorption model (Langmuir isotherm) rather than multilayer sorption model (Freundlich, BET Isotherms). The kinetic study showed that sorption by *RSP* followed a pseudo-second-order kinetic model. Thermodynamic parameters like ΔG° , ΔH° , and ΔS° were also determined. The values indicated the spontaneous nature of adsorption. Enthalpy values showed that the adsorption of Cd(II) was an endothermic process. The comparison of adsorption capacities of *R. sativus* with a number of other adsorbent indicated its effectiveness for Cd(II) adsorption.

Acknowledgments

The authors highly acknowledge the financial assistance from Higher Education Commission, Pakistan for the present work. Some of the research facilities were utilized from Department of Geology and University of Malaya Centre for Ionic Liquids (UMCIL), through research grant HIR UM-MOHE F00004-21001.

References

- [1] IARC, International Agency for Research on Cancer, Monographs on the Evaluation of Carcinogenic Risks of Compounds, vol. 2, IARC, New York, NY, 1976, p. 3976.
- [2] Y. Wang, X. Tang, Y. Chen, L. Zhan, Z. Li, Q. Tang, Adsorption behavior and mechanism of Cd(II) on loess soil from China, *J. Hazard. Mater.* 172 (2009) 30–37.
- [3] J.R. Memon, S.Q. Memon, M.I. Bhangar, M.Y. Khuhawar, G.C. Allen, G.Z. Memon, A.G. Pathan, Efficiency of Cd(II) removal from aqueous media using chemically modified polystyrene foam, *Eur. Polym. J.* 44 (2008) 1501–1511.
- [4] B. Volesky, Detoxification of metal-bearing effluents: Biosorption for the next century, *Hydrometallurgy* 59 (2001) 203–216.
- [5] R. Navarro, S. Wada, K. Tatsumi, Heavy metal precipitation by polycation–polyanion complex of PEI and its phosphonome-thylated derivative, *J. Hazard. Mater.* B123 (2005) 203–209.
- [6] P. Gao, X. Chen, F. Shen, G. Chen, Removal of chromium (VI) from wastewater by combined electrocoagulation–electroflotation without a filter, *Sep. Purif. Technol.* 43 (2004) 117–123.
- [7] S. Lacour, J.C. Bollinger, B. Serpaud, P. Chantron, R. Arcos, Removal of heavy metals in industrial wastewaters by ion-exchanger grafted textiles, *Anal. Chim. Acta* 428 (2002) 121–132.
- [8] H.A. Qdais, H. Moussa, Removal of heavy metals from wastewater by membrane processes: A comparative study, *Desalination*. 164 (2004) 105–110.
- [9] R.A.K. Rao, M.A. Khan, Biosorption of bivalent metal ions from aqueous solution by an agricultural waste: Kinetics, thermodynamics and environmental effects, *Colloids Surf. A: Physicochem. Eng. Asp.* 332 (2009) 121–128.
- [10] M.M. Figueira, B. Volesky, V.S.T. Ciminelli, F.A. Roddick, Biosorption of metals in brown seaweed biomass, *Water Res.* 34 (2000) 196–204.
- [11] M.X. Loukidou, A.I. Zouboulis, Comparison of two biological treatment processes using attached-growth biomass for sanitary landfill leachate treatment, *Environ. Pollut.* 111 (2001) 273–281.
- [12] F. Kirka, N. Azzouz, M.C. Ncibi, Adsorptive removal of cadmium from aqueous solution by cork biomass: Equilibrium, dynamic and thermodynamic studies, *Arab. J. Chem.* (2012). doi:10.1016/j.arabjc.2011.12.013.
- [13] T.K. Sen, M. Mohammad, S. Maitra, B.K. Dutta, Removal of cadmium from aqueous solution using castor seed hull: A kinetic and equilibrium study, *Clean—Soil Air Water* 38 (2010) 850–858.
- [14] S. Çay, A. Uyanık, A. Özaşık, Single and binary component adsorption of copper (II) and cadmium (II) from aqueous solutions using tea-industry waste, *Sep. Purif. Technol.* 38 (2004) 273–280.
- [15] S. Doyurum, A. Çelik, Pb(II) and Cd(II) removal from aqueous solutions by olive cake, *J. Hazard. Mater.* 138 (2006) 22–28.
- [16] A. Chatterjee, S. Schiewer, Biosorption of cadmium (II) ions by citrus peels in a packed bed column: Effect of process parameters and comparison of different breakthrough curve models, *Clean—Soil Air Water* 39 (2011) 874–881.
- [17] L. Semerjian, Equilibrium and kinetics of cadmium adsorption from aqueous solutions using untreated *Pinus halepensis* sawdust, *J. Hazard. Mater.* 173 (2010) 236–242.
- [18] E. Kusvuran, D. Yildirim, A. Samil, O. Gulnaz, A study: Removal of Cu(II), Cd(II) and Pb(II) ions from real industrial water and contaminated water using activated sludge biomass, *Clean—Soil Air Water* 00 (2012) 1–11.
- [19] A. Salmurova, H. Turkmenler, E.E. Ozbas, Biosorption kinetics and isotherm studies of Cd(II) by dried *Enteromorpha compressa* macroalgae cells from aqueous solutions, *Clean—Soil Air Water* 38 (2010) 936–941.
- [20] F.M. Morsy, S.H.A. Hassan, M. Koutb, Biosorption of Cd(II) and Zn(II) by *Nostoc commune*: Isotherm and kinetic studies, *Clean—Soil Air Water* 39 (2012) 680–687.
- [21] D. Mohan, C.U. Pittman, M. Bricka, F. Smith, B. Yancey, J. Mohammad, P.H. Steele, M.F. Alexandre-Franco, V. Gómez-Serrano, H. Gong, Sorption of arsenic, cadmium, and lead by chars produced from fast pyrolysis of wood and bark during bio-oil production, *J. Colloid Interface Sci.* 310 (2007) 57–73.
- [22] E. Fourest, J.C. Roux, Heavy metal biosorption by fungal mycelia by-products: Mechanisms and influence of pH, *Appl. Microbiol. Biotechnol.* 37 (1992) 399–403.
- [23] Q. Li, S. Wu, G. Liu, X. Liao, X. Deng, D. Sun, Y. Hu, Y. Huang, Simultaneous biosorption of cadmium (II) and lead (II) ions by pretreated biomass of *Phanerochaete chrysosporium*, *Sep. Purif. Technol.* 34 (2004) 135–142.
- [24] A. Sari, M. Tuzen, Biosorption of Pb(II) and Cd(II) from aqueous solution using green alga (*Ulva lactuca*) biomass, *J. Hazard. Mater.* 152 (2008) 302–308.
- [25] R. Say, A. Denizli, M.Y. Arica, Biosorption of cadmium (II), lead (II) and copper (II) with the filamentous fungus *Phanerochaete chrysosporium*, *Bioresour. Technol.* 76 (2001) 67–70.
- [26] A. Sari, M. Tuzen, Kinetic and equilibrium studies of biosorption of Pb(II) and Cd(II) from aqueous solution by macrofungus (*Amanita rubescens*) biomass, *J. Hazard. Mater.* 164 (2009) 1004–1011.
- [27] M.A. Kashem, B.R. Sing, S.M.I. Haq, S. Kawai, Fractionation and mobility of cadmium, lead and zinc in some contaminated and non-contaminated soils of Japan, *J. Soil Sci. Environ. Manage.* 2 (2011) 241–249.
- [28] M.J. Iqbal, M.N. Ashiq, Adsorption of dyes from aqueous solutions on activated charcoal, *J. Hazard. Mater.* 139 (2007) 57–66.
- [29] B. Al-Duri, Adsorption modeling and mass transfer, in: G. McKay (Ed.), *Use of Adsorbents for the Removal of Pollutants from Waste Waters*, CRC Press, New York, NY, 1996, pp. 133–173.

- [30] M. Alkan, Ö. Demirbaş, S. Çelikçapa, M. Doğan, Sorption of acid red 57 from aqueous solution onto sepiolite, *J. Hazard. Mater.* 116 (2004) 135–145.
- [31] I.D. Mall, V.C. Sivastava, N.K. Agawal, I.M. Mishra, Removal of congo red from aqueous solution by bagasse fly ash and activated carbon: Kinetic study and equilibrium isotherm analyses, *Chemosphere* 61 (2005) 492–501.
- [32] J.P. Hobson, Physical adsorption isotherms extending from ultrahigh vacuum to vapor pressure, *J. Phys. Chem.* 73 (1969) 2720–2727.
- [33] M.M. Dubinin, L.V. Radushkevich, Equation of the characteristic curve of activated charcoal, *Proc. Acad. Sci. U.S.S.R. Phys. Chem. Sect.* 55 (1947) 331–337.
- [34] J. Li, C.J. Werth, Modeling sorption isotherms of volatile organic chemical mixtures in model and natural solids, *Environ. Toxicol. Chem.* 18 (2002) 1377–1383.
- [35] A.K. Jain, V.K. Gupta, A. Bhatnagar, R. Suhas, Utilization of industrial waste products as adsorbents for the removal of dyes, *J. Hazard. Mater.* 8(101) (2003) 31–42.
- [36] B.H. Hameed, M.I. Al-Khaiary, Removal of basic dye from aqueous medium using a novel agricultural waste material: Pumpkin seed hull, *J. Hazard. Mater.* 155 (2008) 601–609.
- [37] A. Aygun, S. Yenisoay-Karakas, I. Duman, Production of granular activated carbon from fruit stones and nutshells and evaluation of their physical, chemical, and adsorption properties, *Micropor. Mesopor. Mater.* 66 (2003) 189–195.
- [38] L. You, W. Zhijian, T. Kim, K. Lee, Kinetics and thermodynamics of bromophenol blue adsorption by a mesoporous hybrid gel derived from tetraethoxysilane and bis(trimethoxysilyl)hexane, *Colloid Interface. Sci.* 300 (2006) 526–535.
- [39] Z. Bekçi, C. Özveri, Y. Seki, K. Yurdakoç, Sorption of malachite green on chitosan bead, *J. Hazard. Mater.* 154 (2008) 254–261.
- [40] Y.S. Ho, Removal of copper ions from aqueous solution by tree fern, *Water Res.* 37 (2003) 2323–2330.
- [41] C. Aharoni, S. Sideman, E. Hoffer, Adsorption of phosphate ions by collodion-coated alumina, *J. Chem. Technol. Biotechnol.* 29 (1979) 404–412.
- [42] E. Tütem, R. Apak, C.F. Ünal, Adsorptive removal of chlorophenols from water by bituminous shale, *Water Res.* 32 (1998) 2315–2324.
- [43] R. Gong, Y. Sun, J. Chen, H. Liu, C. Yang, Effect of chemical modification on dye adsorption capacity of peanut hull, *Dyes Pigment* 67 (2005) 175–181.